



**HAL**  
open science

## Synthesis and Spectral Properties of 6'-Triazolyl-Dihydroxanthene-Hemicyanine Fused Near-Infrared Dyes

Lingyue Gu, Kévin A Renault, Anthony Romieu, Jean-Alexandre Richard,  
Rajavel Srinivasan

► **To cite this version:**

Lingyue Gu, Kévin A Renault, Anthony Romieu, Jean-Alexandre Richard, Rajavel Srinivasan. Synthesis and Spectral Properties of 6'-Triazolyl-Dihydroxanthene-Hemicyanine Fused Near-Infrared Dyes. *New Journal of Chemistry*, 2020, 44 (28), pp.12208-12215. 10.1039/D0NJ01724H. hal-03230412

**HAL Id: hal-03230412**

**<https://hal.science/hal-03230412>**

Submitted on 19 May 2021

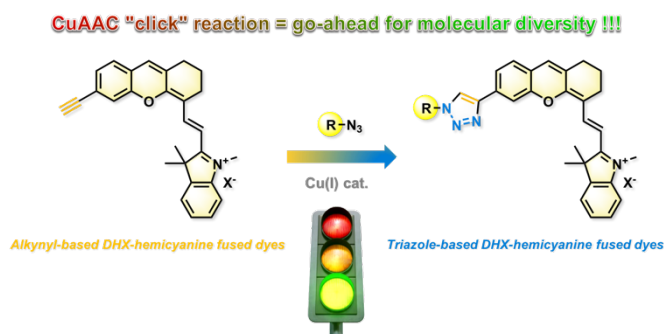
**HAL** is a multi-disciplinary open access archive for the deposit and dissemination of scientific research documents, whether they are published or not. The documents may come from teaching and research institutions in France or abroad, or from public or private research centers.

L'archive ouverte pluridisciplinaire **HAL**, est destinée au dépôt et à la diffusion de documents scientifiques de niveau recherche, publiés ou non, émanant des établissements d'enseignement et de recherche français ou étrangers, des laboratoires publics ou privés.

# Synthesis and Spectral Properties of 6'-Triazolyl-Dihydroxanthene-Hemicyanine Fused Near-Infrared Dyes

Lingyue Gu,<sup>a</sup> Kevin Renault,<sup>b</sup> Anthony Romieu,<sup>\*b</sup> Jean-Alexandre Richard<sup>\*c</sup> and Rajavel Srinivasan<sup>\*a</sup>

We describe the synthesis of a range of 6'-triazolyl-dihydroxanthene-hemicyanine (DHX-hemicyanine) fused dyes through an effective copper-catalyzed azide-alkyne cycloaddition (CuAAC) "click" reaction, with the aim of providing molecular diversity and evaluating spectral properties of these near-infrared (NIR)-active materials. This was implemented by reacting 15 different aliphatic and aromatic azides with a terminal alkynyl-based-DHX-hemicyanine hybrid scaffold prepared in four steps and 35% overall yield from 4-bromosalicylaldehyde. The resulting triazole derivatives have been fully characterized and their optical properties determined both in organic solvents and simulated physiological conditions (phosphate buffered saline containing 5% of bovine serum albumin protein). This systematic study is a first important step towards the development of NIR-I fluorogenic "click-on" dyes or related photoactive agents for light-based diagnostic and/or therapeutic applications.



## Introduction

The essence of "click chemistry" reactions lies in their simplicity, speed and robustness even in aqueous media.<sup>1</sup> While the concept has found popularity in organic chemistry, material science<sup>2</sup> and drug discovery,<sup>3</sup> it comes as no surprise that biologists have also embraced it to perform chemistry in living systems (known as *in vivo* chemistry).<sup>4</sup> By doing so, a new field coined bioorthogonal chemistry emerged and aims at developing advanced chemistry tools for the rational modification of biomolecules helping to a better understand of biology.<sup>5</sup> Of particular interest is the labelling of biomolecules monitoring their activity and leading to the discovery and/or deciphering of new biological mechanisms.

In this context, the association of reactions belonging to the repertoire of "click chemistry" with organic-based fluorophores

has propelled the field of bioorthogonal chemistry to an indispensable tool for the optical imaging of biological systems.<sup>6</sup> For instance, Meldal,<sup>7</sup> Sharpless and co-workers<sup>8</sup> rejuvenated the Huisgen 1,3-cycloaddition<sup>9</sup> and reported a regioselective Cu-catalyzed version (known as CuAAC for copper-catalyzed azide-alkyne cycloaddition) which has become the most iconic "click" reaction known so far.<sup>10</sup> Wang and co-workers applied it to fluorescent molecules and reported CuAAC reaction between 3-azidocoumarins and acetylenes.<sup>11</sup> While the aryl azide precursor did not display any fluorescence properties, the study showed that some of the triazoles formed turned fluorescent. In a similar fashion, Bertozzi's group used an azido aryl moiety as C9-substituent of xanthene-based fluorophores.<sup>12</sup> The initial azido rosamine did not emit any light because of a photoinduced electron transfer (PeT)-mediated quenching process. However, after evaluation of different positions of the azido group and electronic density of the aromatic ring, the fluorescence of the resulting triazole could be enhanced up to 58-fold (Scheme 1A).<sup>13</sup> Kele's group also used aryl azide precursors<sup>14</sup> but the approach using these scaffolds as fluorogenic precursors is limited because of their relative light instability and propensity to form the corresponding nitrene. It is possible to take advantage of this mechanism in the design of photoreactive cross-linkers suitable for photoaffinity labeling<sup>15</sup> but in the context of the development of fluorogenic probes that instability is a serious limitation.<sup>16</sup> One way around the need for an aryl azide precursor is to use a more stable terminal alkynyl-containing fluorophore. When the carbon-carbon triple bond replaces electron-donating groups (typically, *N,N*-dialkylamino moieties) it can turn the fluorophore to weakly or not fluorescent. This strategy was demonstrated by Tung's group on benzothiazoles<sup>17</sup> and by Yao and co-workers on

<sup>a</sup> G. Lingyue, Prof. R. Srinivasan  
School of Pharmaceutical Science and Technology (SPST), Tianjin University,  
Building 24, 92 Weijin Road, Nankai District, Tianjin, 300072 P. R. China  
E-mail: rajavelst@tju.edu.cn

<sup>b</sup> Dr. K. Renault, Prof. A. Romieu  
ICMUB, UMR 6302, CNRS, Univ. Bourgogne Franche-Comté  
9, Avenue Alain Savary, 21000 Dijon, France  
E-mail: anthony.romieu@u-bourgogne.fr

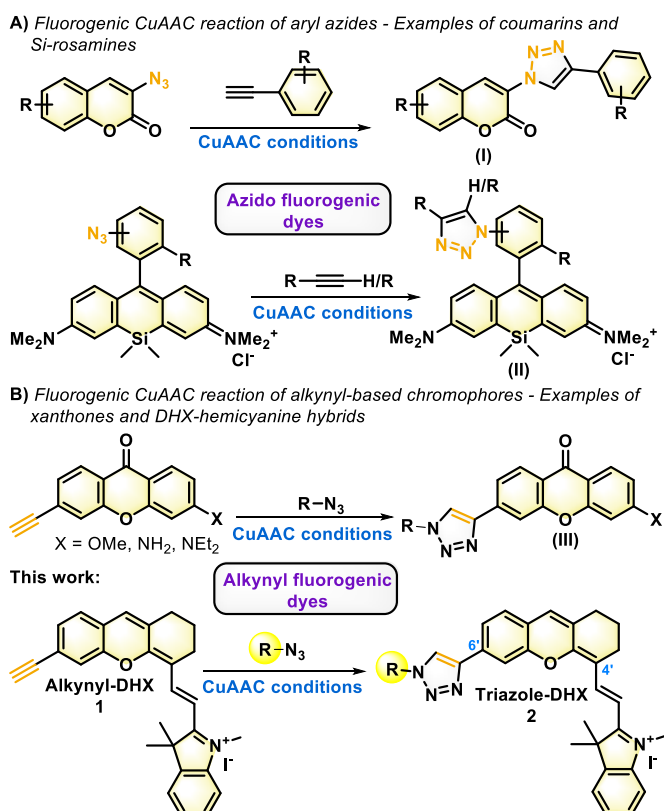
<sup>c</sup> Dr. J.-A. Richard  
Functional Molecules and Polymers  
Institute of Chemical and Engineering Sciences (ICES), Agency for Science,  
Technology and Research (A\*STAR)  
8 Biomedical Grove, Neuros, #07-01, Singapore 138665  
E-mail: jean\_alexandre@ices.a-star.edu.sg

†Electronic Supplementary Information (ESI) available: Protocols, NMR and HMRS data as well as copies of NMR spectra, HPLC traces and selected UV and fluorescence spectra.

rosamine- and xanthone-based fluorophores which displayed an increase of fluorescence emission upon formation of the triazole ring (Scheme 1B).<sup>18</sup>

Despite the advantages of longer-wavelength fluorescence light, known to facilitate molecular imaging in complex biological systems,<sup>19</sup> such strategies have mostly been implemented with fluorophores emitting in the visible spectral range and little progress has been made so far on the development of similar near-infrared (NIR)-emitting dyes (specifically, within NIR-I optical window 650-900 nm). Over the years, our respective groups have designed chemical methods leading to the development of a novel class of NIR-I dyes based on a molecular hybrid scaffold that combine both structural features of xanthene and cyanine parent compounds.<sup>20</sup> These dihydroxanthene (DHX)-hemicyanine fused fluorophores are now regarded as attractive alternatives to the popular and commonly used polymethine-cyanine dyes, as illustrated by numerous and valuable achievements in the fields of biosensing, bioimaging and theranostics.<sup>21</sup> Attracted by the modularity and ease of chemical modification of DHX-hemicyanine hybrid dyes, we set out to develop the access to a DHX precursor allowing the facile "click" formation of triazoles.

In a first attempt toward this goal, the introduction of an azido group on the 6'-position of the DHX skeleton proved to be a dead-end because of the marked photosensitivity of the aryl azide obtained. Instead, we took inspiration from our previous work to prepare an alkynyl-based DHX precursor **1** from the corresponding aryl bromide.<sup>22</sup> We then explored CuAAC reaction with aliphatic and aromatic azides. Finally, we determined the spectral properties of the resulting "clicked" fluorophores **2a-2o** to assess the influence of both triazole moiety and its substitution pattern on NIR absorption/emission ability of fused DHX-hemicyanine scaffold (Scheme 1B). Details of these investigations and their possible extensions are discussed in the present Article.

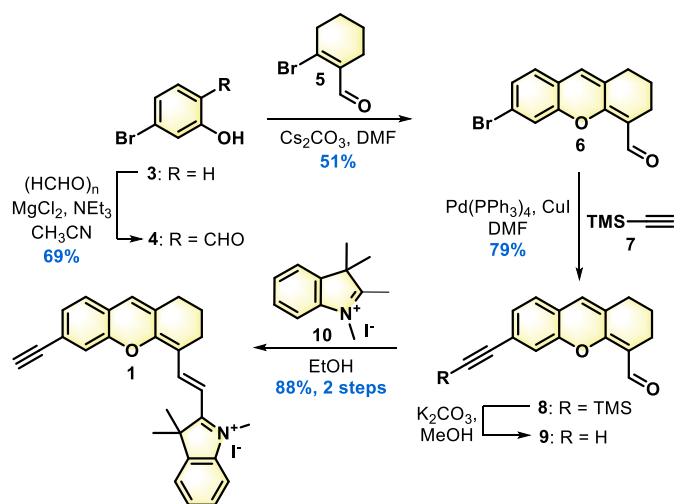


**Scheme 1** CuAAC reaction for the development of fluorogenic "click-on" dyes. A) Reaction of 3-azidocoumarin and Si-rosamine fluorogenic dyes with terminal alkynes; B) Reaction of alkynyl-based xanthone and DHX fluorogenic dyes with azido compounds.

## Results and discussion

### Synthesis of a library of 6'-triazolyl-dihydroxanthene-hemicyanine fused dyes

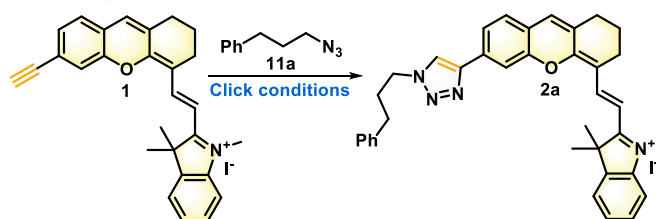
We started our study with the preparation of the alkyne "click" partner **1** which we readily obtained in two steps from bifunctional arylbrominated aldehyde **6** (Scheme 2). This latter DHX-hemicyanine precursor was prepared in two steps from 3-bromophenol **3** through (1) Casnati-Skattebøl *ortho*-formylation ( $\text{MgCl}_2$ ,  $(\text{HCHO})_n$ ,  $\text{NEt}_3$ )<sup>23</sup> that provided 4-bromosalicylaldehyde **4** in 69% yield, and its subsequent (2) one-pot reaction with enal **5** to form the DHX skeleton **6**. The aryl bromide moiety was then reacted with trimethylsilylacetylene **7** under Sonogashira reaction conditions ( $\text{Pd}(\text{PPh}_3)_4$ ,  $\text{CuI}$ , 79% yield).<sup>22</sup> After removal of the TMS group under conventional conditions ( $\text{K}_2\text{CO}_3$ ,  $\text{CH}_3\text{OH}$ ), the formyl group was reacted with 1,2,3,3-tetramethyl-3*H*-indol-1-ium iodide (Fisher's base) **10** to yield the desired alkynyl-based DHX-hemicyanine fused dye **1** in 88% yield over two steps. The structure was proven by NMR and ESI mass analyses and the high level of purity (>94% whatever the wavelength used for the UV-vis detection) was confirmed by RP-HPLC-based analytical control (see ESI†).



**Scheme 2** Preparation of the alkenyl-based DHX-hemicyanine fused dye **1** in five steps from 3-bromophenol **3**.

We next explored reaction conditions allowing the formation of the desired triazole ring at the 6' position of the DHX-hemicyanine fused dye (Scheme 3A). To this end, we optimized the reaction conditions at room temperature in the presence of (3-azidopropyl)benzene **11a** as azido "click" partner, sodium ascorbate and various copper sources. While the use of copper(II) chloride and copper(II) sulfate pentahydrate provided some product (10% and 13% yield, respectively, Scheme 3A, entries 1-2), copper(II) acetate, copper(II) triflate and copper(I) chloride were much less successful (Scheme 3A, entries 3-6). Other usual "click" conditions using copper(I) sources without sodium ascorbate didn't provide any promising result either (Scheme 3A, entries 6 and 9). However, switching from the commonly used *tert*-butanol/water mixture of solvent to pure water in the presence of sodium ascorbate improved the yield significantly from 13% to 38% (Scheme 3A, entries 2 and 7). Ultimately, a mixture of DCM and water (Scheme 3A, entry 8) and 10 h reaction time appeared to be optimal (Scheme 3A, entries 10-12). With an interesting 50% yield (Scheme 3A, entry 8) it allowed us to explore the scope of the reaction with a wide range of alkyl and aryl azides **11b-o** (see ESI<sup>+</sup> for their synthesis).

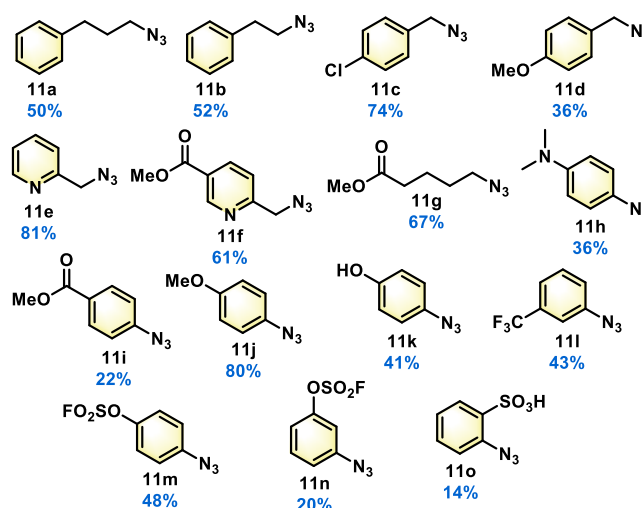
**A) Screening of reaction conditions for CuAAC**



Entry	Solvent	Catalyst	Additive	Time (h)	Yield (%) <sup>[a]</sup>
1	DCM/H <sub>2</sub> O (1:1)	CuCl <sub>2</sub>	Na ascorbate	10	10
2	<i>t</i> BuOH/H <sub>2</sub> O	CuSO <sub>4</sub> · 5H <sub>2</sub> O	Na ascorbate	10	13
3	THF	Cu(OAc) <sub>2</sub>	Na ascorbate	10	0
4	THF	Cu(OTf) <sub>2</sub>	Na ascorbate	10	Trace
5	EtOH	Cu(OTf) <sub>2</sub>	Na ascorbate	10	Trace
6	CH <sub>3</sub> CN	CuCl	NEt <sub>3</sub>	10	0
7	H <sub>2</sub> O	CuSO <sub>4</sub> · 5H <sub>2</sub> O	Na ascorbate	10	38
8	DCM/H <sub>2</sub> O (1:1)	CuSO <sub>4</sub> · 5H <sub>2</sub> O	Na ascorbate	10	50
9	DCM/H <sub>2</sub> O (1:1)	CuI	NEt <sub>3</sub>	10	0
10	DCM/H <sub>2</sub> O (1:1)	CuSO <sub>4</sub> · 5H <sub>2</sub> O	Na ascorbate	6	36
11	DCM/H <sub>2</sub> O (1:1)	CuSO <sub>4</sub> · 5H <sub>2</sub> O	Na ascorbate	8	45
12	DCM/H <sub>2</sub> O (1:1)	CuSO <sub>4</sub> · 5H <sub>2</sub> O	Na ascorbate	12	50

[a] Yield after purification by column chromatography over silica gel

**B) Scope of the synthesis of triazole-based DHX-hemicyanine hybrids**



**Scheme 3** A) Optimization of the CuAAC reaction for the synthesis of 6'-triazolyl-DHX-hemicyanine fused dyes **2**; B) Scope of the CuAAC reaction using aliphatic and aromatic azides.

With one less carbon in its alkyl chain, (2-azidoethyl)benzene **11b** behaved similarly to azide **11a** and formed the corresponding triazole **2b** in 52% yield. 4-Chloro- and 4-methoxybenzyl azide **11c** and **11d** were also successful (the corresponding triazoles **2c** and **2d** were isolated in 74% and 36% yields, respectively) and the two 2-(azidomethyl)pyridines **11e** and **11f** developed by the Ting group to speed-up the CuAAC reaction *in cellulo* gave triazole cycloadducts **2e** and **2f** in good 81% and 61% yields, respectively.<sup>24</sup> The availability of triazole-based fluorophores bearing an extra functional group for structural tuning or covalent conjugation to other (bio)molecular partners is of great interest for biological applications. The CuAAC reaction was therefore achieved with **11g**, **11i**, **11m** and **11n** to introduce either a latent carboxylic acid (masked as methyl ester) or an aryloxysulfonyl fluoride moiety (this latter one being identified as an effective reactive

partner in "click" reaction sulfur(VI) fluoride exchange (SuFEx)<sup>25</sup>). The possible influence of an electron-donating or -withdrawing substituent introduced on triazole moiety, over spectral properties of the resulting "clicked" DHX-based dyes, was also addressed through the successful synthesis of **2h-2l**. Finally, the presence of an *ortho*-substituted sulfonic acid group in **11o** provided a simple way to introduce a polar group facilitating the water-solubilization of the resulting DHX-hemicyanine fused dye **2o** (Scheme 3B). The structures of these 15 novel triazole-based DHX-hemicyanine fused dyes were unambiguously confirmed by ESI-HRMS and NMR spectroscopic analyses (see ESI<sup>†</sup>). Their purity was checked by RP-HPLC and found to be above 95%, value usually required to achieve relevant photophysical measurements.

### Photophysical properties of 6'-triazolyl-dihydroxanthene-hemicyanine fused dyes

To assess changes in photophysical properties after triazole formation, we next studied the spectral behavior of our library of 15 DHX-hemicyanine fused dyes **2a-2o** and alkyne precursor **1** in different media including phosphate buffered saline (PBS) with 5% (w/v) bovine serum albumin (BSA) as simulated body fluid, EtOH, and CHCl<sub>3</sub> (Table 1 and Fig. 1 for the Abs/Ex/Em spectra of **1** and **2o** in CHCl<sub>3</sub> and in PBS + 5% BSA, see ESI<sup>†</sup> for Abs/Ex/Em spectra of other compounds). A first general trend common to all triazole-based dyes and alkyne **1** is the dramatic broadening of the main absorption band assigned to S<sub>0</sub>-S<sub>1</sub> electronic transition, compared to that of more conventional DHX-hemicyanine fused fluorophore bearing a *N,N*-dialkylamino group as C-6' substituent like **12**, which explains the notable lower molar extinction coefficient of dyes **2a-2o** compared to **12**. A full-width half maximum (FWHM),  $\Delta\lambda_{1/2 \text{ max}}$  in the range of 3410-4370 cm<sup>-1</sup> is observed depending primarily on the solvent used, against only 695-990 nm for **12** and unlike the latter, well-defined vibronic structures with two maxima and one pronounced blue-shifted shoulder are observed in all absorption spectra. The lack of an effective electron-donating group such as -NEt<sub>2</sub>, on C-6' position, induces an expected hypsochromic shift of ca. 50 nm or 100 nm depending the local absorption maximum regarded for the triazole derivatives, of the maximum absorption peak position for the DHX-hemicyanine hybrid scaffold. This feature also contributes to the dramatic decrease of molar extinction coefficients compared to those of more conventional DHX-based fluorophores such as **12**.

Red excitation at 620 nm produced the desired NIR emission in the form of a vibronic structure with two well-defined maxima in the range 690-760 nm. However, only a very weak fluorescence emission intensity was observed, whatever the triazole derivative studied, the solvent and concentration range (1-10 μM) used. It prevented us to accurately determine relative fluorescence quantum yields, roughly

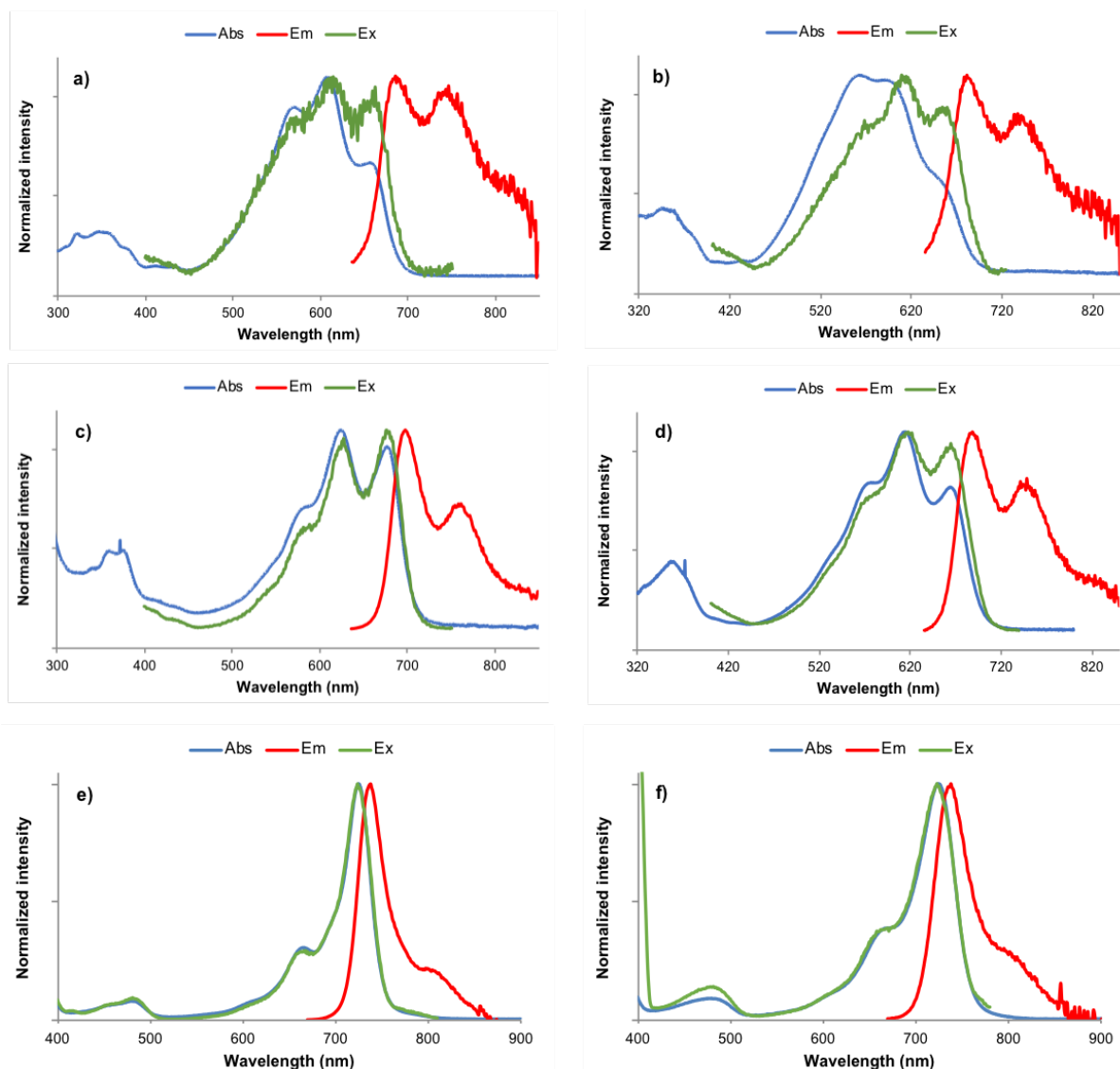
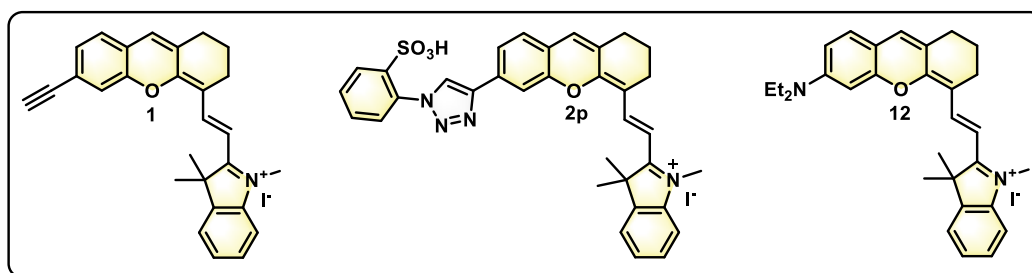


**Fig. 1** Normalised absorption, emission (excitation at 620 nm for a-d and 650 nm for e-f) and excitation (emission at 760 nm for a-d, 830 nm for e or 800 nm for f) spectra of alkynyl-based DHX-hemicyanine fused dye **1** (a in  $\text{CHCl}_3$  and b in  $\text{PBS} + 5\% \text{BSA}$ ), triazole-based DHX-hemicyanine fused dye **2o** (c in  $\text{CHCl}_3$  and d in  $\text{PBS} + 5\% \text{BSA}$ ), and *N,N*-diethylamino-DHX-hemicyanine fused dye **12** (e in  $\text{CHCl}_3$  and f in  $\text{PBS} + 5\% \text{BSA}$ ). For the excitation spectrum of **12** in  $\text{PBS} + 5\% \text{BSA}$ , a peak at 400 nm ( $\lambda_{\text{ex}}/2$ ) assigned to Rayleigh scattering is observed. See the Experimental section for details about these measurements.

estimated at less than 1%. The very low values of these quantum yields cannot be attributed to the formation of non-emissive aggregates (*i.e.*, H-type homodimers)<sup>26</sup> because a good matching between the absorption and excitation spectra was observed except for some triazole derivatives (*e.g.*, **2i**, **2l** and **2m**, see ESI<sup>+</sup>) and **1** spectrally characterised in simulated physiological conditions (*i.e.*,

$\text{PBS} + 5\% \text{BSA}$ ). The capability of BSA protein to disrupt fluorophore aggregates in aq. media is well-documented but in the present case, its surfactant behavior was not sufficiently effective to obtain a single emissive species in solution.<sup>27</sup> Alternatively, we attempted to assess the relative fluorescence efficiency of dyes **2a-2o** and **1** by calculating the ratio [(integration of emission curve)/absorption at 620 nm] for

a single concentration (5  $\mu$ M) solution in  $\text{CHCl}_3$  of each compound (**1** and **2a-2o**). We observed a change in color of solution from sapphire blue (for alkyne **1**) to sky blue (for triazole derivatives **2a-2o**) (see ESI<sup>†</sup>) but could not obtain reliable values allowing an accurate and relevant ranking of the fluorophores synthesized in this study, based on their emissive capability.

## Conclusions

Quest for high-performance NIR-I chromophores/fluorophores based on the attractive DHX-hemicyanine hybrid scaffold led us to consider for the first time CuAAC "click" reaction as a simple way of achieving high molecular diversity through the straightforward synthesis of alkynyl-based DHX-hemicyanine fused dye **1** and its "click" derivatisation with a wide range of organic azides. In contrast to already published fluorogenic alkynes photoactive in the blue-green spectral range, only a weak fluorescence emission of triazole-based dyes was observed within the NIR-I window. Thus, our efforts that involved synthesis and photophysical characterization of a library of 15 different compounds will require a further structural optimization to obtain NIR-I fluorogenic "click-on" dyes suitable for bioimaging. Interestingly, the specific molecular absorption signature of both alkyne and triazole derivatives (*i.e.*, broad, structured and weakly solvent dependent absorption band) might be used to design novel broad spectrum dark quencher molecules suitable for the construction of far-red or NIR-I fluorescence light-up probes based on Förster resonance energy transfer (FRET) mechanism.<sup>28</sup>

## Experimental<sup>†</sup>

See ESI<sup>†</sup> for the details about sections "General", "Instruments and methods", and all experimental and spectral data associated with synthesised compounds.

### Synthesis

**6-((Trimethylsilyl)ethynyl)-2,3-dihydro-1H-xanthene-4-carbaldehyde (8).** Pd(PPh<sub>3</sub>)<sub>4</sub> (67.5 mg, 8.3 mmol%) and CuI (23.6 mg, 0.1 mmol) were degassed in a flame-dried round bottom flask. NEt<sub>3</sub> (1.2 mL, 8.3 mmol) in dry DMF (10 mL) was added with aryl bromide **6** (1.2 g, 4.1 mmol). The solution was degassed again then trimethylsilylacetylene **7** was added (1.8 mL, 12.4 mmol). The reaction mixture was heated to 85 °C for 24 h. After being cooled to room temperature, the reaction mixture was concentrated under vacuum and the resulting residue was purified by flash-column chromatography on silica gel (eluent: 1% EtOAc in PE) affording pure TMS-protected terminal alkyne **8** as an orange solid (1.0 g, yield 79%). <sup>1</sup>H NMR (400 MHz, CDCl<sub>3</sub>):  $\delta$  = 10.30 (s, 1 H), 7.17 (s, 1 H), 7.13 (dd,  $J$  = 7.8 Hz,  $J$  = 1.2 Hz, 1 H), 7.05 (d,  $J$  = 7.8 Hz, 1 H), 6.62 (s, 1 H), 2.58 (ddd,  $J$  = 7.5 Hz,  $J$  = 5.8 Hz,  $J$  = 1.6 Hz, 2 H), 2.43 (t,  $J$  = 6.0 Hz, 2 H), 1.71 (m, 2 H), 0.25 (s, 9 H); <sup>13</sup>C NMR (101 MHz, CDCl<sub>3</sub>):  $\delta$  = 188.0, 159.9, 151.7, 130.8, 127.6, 126.5, 126.1, 124.6, 121.6, 118.6, 113.8, 104.0, 96.9, 30.3, 21.6, 20.4, 0.0 ppm; HRMS (ESI<sup>+</sup>):  $m/z$  331.1141 [M + Na]<sup>+</sup>, calcd for C<sub>19</sub>H<sub>20</sub>O<sub>2</sub>SiNa<sup>+</sup> 331.1125.

**6-Ethynyl-2,3-dihydro-1H-xanthene-4-carbaldehyde (9).** TMS-protected terminal alkyne **8** (1.0 g, 3.3 mmol) was dissolved in dry MeOH (30 mL) and treated with anhydrous K<sub>2</sub>CO<sub>3</sub> (1.8 g, 13.2 mmol). The mixture was stirred at room temperature for 5 h. The solvent was removed, and the residue was taken up in 100 mL of DCM and washed with 100 mL of deionised water. The organic layer was dried over anhydrous Na<sub>2</sub>SO<sub>4</sub> and concentrated under reduced pressure. This compound was used in the next step without further purification, and the yield was assumed to be quantitative. <sup>1</sup>H NMR (400 MHz, DMSO-*d*<sub>6</sub>):  $\delta$  = 10.26 (s, 1 H), 7.36 (d,  $J$  = 7.9 Hz, 1 H), 7.34 (s, 1 H), 7.24 (dd,  $J$  = 7.8 Hz,  $J$  = 1.5 Hz, 1 H), 7.01 (s, 1 H), 4.37 (s, 1 H), 2.59 (ddd,  $J$  = 7.0 Hz,  $J$  = 5.3 Hz,  $J$  = 1.6 Hz, 2 H), 2.30 (t,  $J$  = 6.0 Hz, 2 H), 1.63 (m, 2 H) ppm; <sup>13</sup>C NMR (101 MHz, CDCl<sub>3</sub>):  $\delta$  = 188.1, 159.8, 151.7, 131.1, 127.7, 126.6, 125.9, 123.6, 122.0, 118.9, 113.9, 82.8, 79.3, 30.3, 21.6, 20.4 ppm; HRMS (ESI<sup>+</sup>):  $m/z$  237.0910 [M + H]<sup>+</sup>, calcd for C<sub>16</sub>H<sub>13</sub>O<sub>2</sub><sup>+</sup> 237.0910.

**Alkynyl-based DHX-hemicyanine fused dye (1).** To aldehyde **9** (236 mg, 1.0 mmol) in EtOH (2 mL) was added 1,2,3,3-tetramethyl-3H-indol-1-ium iodide **10** (301 mg, 1.0 mmol) and the solution was refluxed at 80 °C for 4 h. The reaction mixture was concentrated and the crude product was purified by flash-column chromatography on silica gel (eluent: 1% MeOH in DCM) to afford alkynyl-DHX **1** as a dark blue solid (345 mg, yield 88%). m.p. >300 °C; <sup>1</sup>H NMR (400 MHz, DMSO-*d*<sub>6</sub>):  $\delta$  = 8.56 (d,  $J$  = 15.3 Hz, 1 H), 7.80-7.73 (m, 2 H), 7.62 (s, 1 H), 7.58 (m, 1 H), 7.52 (m, 2 H), 7.39-7.33 (m, 2 H), 6.68 (d,  $J$  = 15.4 Hz, 1 H), 4.52 (s, 1 H), 3.95 (s, 3 H), 2.72 (t,  $J$  = 6.0 Hz, 2 H), 2.67 (t,  $J$  = 6.0 Hz, 2 H), 1.83 (m, 2 H), 1.77 (s, 6 H) ppm; <sup>13</sup>C NMR (101 MHz, DMSO-*d*<sub>6</sub>):  $\delta$  = 179.0, 158.0, 151.8, 145.1, 142.4, 142.1, 131.1, 129.8, 128.8, 128.4, 127.8, 127.6, 123.8, 122.6, 122.2, 118.6, 114.3, 113.8, 107.2, 83.8, 82.6, 50.8, 33.2, 28.7, 26.9, 23.5, 19.7 ppm; HRMS (ESI<sup>+</sup>):  $m/z$  392.2019 [M]<sup>+</sup>, calcd for C<sub>28</sub>H<sub>26</sub>NO<sup>+</sup> 392.2009; HPLC (system A):  $t_R$  = 4.9 min (purity 94% at 260 nm and 98% at 600 nm); LRMS (ESI<sup>+</sup>, recorded during RP-HPLC analysis):  $m/z$  392.3 [M]<sup>+</sup> (100), calcd for C<sub>28</sub>H<sub>26</sub>NO<sup>+</sup> 392.2; UV-vis (recorded during the HPLC analysis):  $\lambda_{\text{max}}$  = 559 and 592 nm (broad band).

**General procedure for the synthesis of tetrazole-based DHX-hemicyanine fused dyes 2a-2o.** To a mixture of alkynyl-based DHX-hemicyanine dye **1** (784 mg, 2.0 mmol, 1.0 equiv.) and the corresponding organic azide **11a-o** (2.6 mmol, 1.3 equiv.) in deionised water and CH<sub>2</sub>Cl<sub>2</sub> (1:1 (v/v), 100 mL), sodium ascorbate (79.2 mg, 0.4 mmol, 0.2 equiv.) was added, followed by the addition of CuSO<sub>4</sub> • 5 H<sub>2</sub>O (25 mg, 0.1 mmol, 0.05 equiv.). The heterogeneous mixture was stirred vigorously at room temperature overnight. Thereafter, the reaction mixture was concentrated under reduced pressure and directly purified by flash-column chromatography on silica gel (eluent: 1% MeOH in DCM) to afford the corresponding triazole **2a-2o** as a dark blue amorphous powder.

### Photophysical characterisations

UV-visible spectra were obtained either on a Varian Cary 50 scan (single-beam) or an Agilent technologies 60 (single-beam) spectrophotometer (software Cary WinUV) by using rectangular quartz cells (Hellma, 100-QS, 45 × 12.5 × 12.5 mm, pathlength: 10 mm, chamber volume: 3.5 mL), at 25 °C (using a temperature control system combined with water circulation). Fluorescence spectra (emission/excitation spectra) were recorded with an HORIBA Jobin Yvon Fluorolog spectrofluorometer (FluorEssence software) at 25 °C (using a temperature control system combined with water circulation), with standard fluorometer

cells (Labbox, LB Q, light path: 10 mm, width: 10 mm, chamber volume: 3.5 mL). The absorption and fluorescence emission spectra were recorded with dye solutions of concentrations in the range of  $10^{-5}$ - $10^{-6}$  M. The emission spectra were recorded in the range of 635-850 nm after excitation at 620 nm (shutter: Auto Open, integration time = 0.1 s, 1 nm step, HV(S1) = 950 V, excitation slit = 5 nm and emission slit = 5 nm). The excitation spectra were recorded in the range of 400-750 nm after emission at 760 nm (excitation slit = 5 nm for spectra recorded in  $\text{CHCl}_3$  and 12 nm for spectra recorded in EtOH or PBS + 5% BSA and emission slit = 5 nm). All excitation/emission spectra are corrected.

## Conflicts of interest

The authors declare no conflict of interest.

## Acknowledgements

This work is supported by SPST, Tianjin University (P.R. China), ICES, A\*STAR (Singapore), and the CNRS, Université de Bourgogne and Conseil Régional de Bourgogne through the "Plan d'Actions Régional pour l'Innovation (PARI) and the "Fonds Européen de Développement Régional (FEDER)" programs. Financial supports from Agence Nationale de la Recherche (ANR, AAPG 2018, PRCI LuminoManufacOligo, ANR-18-CE07-0045-01), especially for the post-doc fellowship of K. R., the National Research Foundation Singapore (NRF, LuminoManufacOligo, NRF2018-NRF-ANR035) and GDR CNRS "Agents d'Imagerie Moléculaire" (AIM) 2037 are also greatly acknowledged. The authors thank Ms Doris Tan (ICES, Singapore) and Dr. Quentin Bonnin (CNRS, PACSMUB) for the recording of HRMS spectra. A. R. and K. R thank the "Plateforme d'Analyse Chimique et de Synthèse Moléculaire de l'Université de Bourgogne" (PACSMUB, <http://www.wpcm.fr>) for access to spectroscopy instrumentation.

## Notes and references

- 1 H. C. Kolb, M. G. Finn and K. B. Sharpless, *Angew. Chem. Int. Ed.*, 2001, **40**, 2004.
- 2 (a) J.-F. Lutz, *Angew. Chem. Int. Ed.*, 2007, **46**, 1018; (b) H. Nandivada, X. Jiang and J. Lahann, *Adv. Mater.*, 2007, **19**, 2197.
- 3 H. C. Kolb and K. B. Sharpless, *Drug Discov. Today*, 2003, **8**, 1128.
- 4 (a) J. A. Prescher and C. R. Bertozzi, *Nat. Chem. Biol.*, 2005, **1**, 13; (b) M. Boyce and C. R. Bertozzi, *Nat. Methods*, 2011, **8**, 638; (c) C. R. Bertozzi and P. Wu, *Curr. Opin. Chem. Biol.*, 2013, **17**, 717; (d) J. G. Rebelein and T. R. Ward, *Curr. Opin. Biotechnol.*, 2018, **53**, 106.
- 5 (a) J. M. Baskin and C. R. Bertozzi, *QSAR & Comb. Sci.*, 2007, **26**, 1211; (b) E. M. Sletten and C. R. Bertozzi, *Angew. Chem. Int. Ed.*, 2009, **48**, 6974; (c) E. M. Sletten and C. R. Bertozzi, *Acc. Chem. Res.*, 2011, **44**, 666.
- 6 (a) C. Le Droumaguet, C. Wang and Q. Wang, *Chem. Soc. Rev.*, 2010, **39**, 1233; (b) P. Shieh and C. R. Bertozzi, *Org. Biomol. Chem.*, 2014, **12**, 9307.
- 7 (a) C. W. Tornøe, C. Christensen and M. Meldal, *J. Org. Chem.*, 2002, **67**, 3057; (b) M. Meldal and C. W. Tornøe, *Chem. Rev.*, 2008, **108**, 2952.
- 8 V. V. Rostovtsev, L. G. Green, V. V. Fokin and K. B. Sharpless, *Angew. Chem. Int. Ed.*, 2002, **41**, 2596.
- 9 R. Huisgen, *Proc. Chem. Soc.*, 1961, 357.
- 10 D. Brunel and F. Dumur, *New J. Chem.*, 2020, **44**, 3546.
- 11 K. Sivakumar, F. Xie, B. M. Cash, S. Long, H. N. Barnhill and Q. Wang, *Org. Lett.*, 2004, **6**, 4603.
- 12 (a) P. Shieh, M. J. Hangauer and C. R. Bertozzi, *J. Am. Chem. Soc.*, 2012, **134**, 17428; (b) P. Shieh, V. T. Dien, B. J. Beahm, J. M. Castellano, T. Wyss-Coray and C. R. Bertozzi, *J. Am. Chem. Soc.*, 2015, **137**, 7145.
- 13 P. Shieh, M. S. Siegrist, A. J. Cullen and C. R. Bertozzi, *Proc. Natl. Acad. Sci. U S A*, 2014, **111**, 5456.
- 14 (a) A. Herner, I. Nikić, M. Kállay, E. A. Lemke and P. Kele, *Org. Biomol. Chem.*, 2013, **11**, 3297; (b) G. B. Cserép, A. Herner and P. Kele, *Methods Appl. Fluoresc.*, 2015, **3**, 042001; (c) Z. Pünkösti, P. Kele and A. Herner, *J. Het. Chem.*, 2018, **55**, 1183.
- 15 G. T. Hermanson, in *Bioconjugate Techniques (Third Edition)*, Academic Press, Boston, 2013, ch. 3, pp. 253.
- 16 E. Păunescu, L. Louise, L. Jean, A. Romieu and P.-Y. Renard, *Dyes Pigm.*, 2011, **91**, 427.
- 17 (a) J. Qi and C.-H. Tung, *Bioorg. Med. Chem. Lett.*, 2011, **21**, 320; (b) J. Qi, M.-S. Han, Y.-C. Chang and C.-H. Tung, *Bioconjugate Chem.*, 2011, **22**, 1758.
- 18 J. Li, M. Hu and S. Q. Yao, *Org. Lett.*, 2009, **11**, 3008.
- 19 (a) R. Weissleder and U. Mahmood, *Radiology*, 2001, **219**, 316; (b) J. V. Frangioni, *Curr. Opin. Chem. Biol.*, 2003, **7**, 626; (c) I. Martinić, S. V. Eliseeva and S. Petoud, *J. Lumin.*, 2017, **189**, 19.
- 20 (a) J.-A. Richard, *Org. Biomol. Chem.*, 2015, **13**, 8169; (b) A. Romieu and J.-A. Richard, *Tetrahedron Lett.*, 2016, **57**, 317; (c) M. J. H. Ong, S. Debieu, M. Moreau, A. Romieu and J.-A. Richard, *Chem. Asian J.*, 2017, **12**, 936; (d) S. Zheng, G. Lingyue, M. J. H. Ong, D. Jacquemin, A. Romieu, J.-A. Richard and R. Srinivasan, *Org. Biomol. Chem.*, 2019, **17**, 4291.
- 21 H. Chen, B. Dong, Y. Tang and W. Lin, *Acc. Chem. Res.*, 2017, **50**, 1410.
- 22 M. J. H. Ong, R. Srinivasan, A. Romieu and J.-A. Richard, *Org. Lett.*, 2016, **18**, 5122.
- 23 (a) N. U. Hofsløkken and L. Skattebøl, *Acta Chem. Scand.*, 1999, **53**, 258; (b) T. V. Hansen and L. Skattebøl, *Org. Synth.*, 2005, **82**, 64; (c) T. V. Hansen and L. Skattebøl, *Org. Synth.*, 2012, **89**, 220.
- 24 C. Uttamapinant, A. Tangepeerachakul, S. Grecian, S. Clarke, U. Singh, P. Slade, K. R. Gee and A. Y. Ting, *Angew. Chem. Int. Ed.*, 2012, **51**, 5852.
- 25 (a) J. Dong, L. Krasnova, M. G. Finn and K. B. Sharpless, *Angew. Chem. Int. Ed.*, 2014, **53**, 9430; (b) A. S. Barrow, C. J. Smedley, Q. Zheng, S. Li, J. Dong and J. E. Moses, *Chem. Soc. Rev.*, 2019, **48**, 4731; (c) A. Marra, C. Nativi and A. Dondoni, *New J. Chem.*, 2020, **44**, 4678.
- 26 M. Ogawa, N. Kosaka, P. L. Choyke and H. Kobayashi, *ACS Chem. Biol.*, 2009, **4**, 535.
- 27 Pauli, M. Grabolle, R. Brehm, M. Spieles, F. M. Hamann, M. Wenzel, I. Hilger and U. Resch-Genger, *Bioconjugate Chem.*, 2011, **22**, 1298.
- 28 (a) T. Myochin, K. Hanaoka, S. Iwaki, T. Ueno, T. Komatsu, T. Terai, T. Nagano and Y. Urano, *J. Am. Chem. Soc.*, 2015, **137**, 4759; (b) J. Demuth, R. Kucera, K. Kopecky, Z. Havlínová, A. Libra, V. Novakova, M. Miletin and P. Zimcik, *Chem. Eur. J.*, 2018, **24**, 9658.



**Table 1** Photophysical properties of alkynyl-based DHX-hemicyanine fused dye **1**, triazole derivatives **2a-2o** and reference dye **12**<sup>22</sup> at 25 °C. For structures, see ESI†.

Entry	Dye	Abs max <sup>a</sup> [nm]			Em max <sup>c,d</sup> [nm]			$\epsilon$ [M <sup>-1</sup> cm <sup>-1</sup> ]			Stokes' shift <sup>e</sup> [cm <sup>-1</sup> ]		
		CHCl <sub>3</sub>	EtOH	PBS <sup>b</sup>	CHCl <sub>3</sub>	EtOH	PBS	CHCl <sub>3</sub>	EtOH	PBS	CHCl <sub>3</sub>	EtOH	PBS
1	<b>1</b>	569	562	566	685	675	681	25 700	38 750	31 150	1876	1935	2038
		607	597	598	746	728	741	45 200	42 200	31 000			
		654	640	645				38 300	22 850	16 700			
2	<b>2a</b>	579	572	578	693	686	688	34 200	35 200	28 600	1777	1870	1752
		617	608	614	755	741	751	52 050	44 200	34 550			
		670	656	662				40 600	28 200	22 500			
3	<b>2b</b>	579	573	575	691	685	687	41 800	42 100	35 700	1683	1849	1784
		619	608	612	755	742	748	63 500	53 100	41 250			
		671	656	661				48 600	33 700	26 450			
4	<b>2c</b>	579	571	573	692	684	688	38 100	45 100	36 700	1730	1854	1805
		618	607	612	752	744	747	58 900	56 450	39 300			
		670	656	662				45 800	35 500	25 300			
5	<b>2d</b>	579	571	573	693	685	686	40 400	44 250	38 500	1751	1849	1789
		618	608	611	754	749	748	59 050	55 850	41 000			
		670	656	663				43 500	35 600	27 050			
6	<b>2e</b>	580	572	570	694	685	688	42 100	43 050	38 950	1720	1876	1939
		620	607	607	751	745	741	62 200	54 150	35 700			
		671	656	661				46 100	34 200	23 350			
7	<b>2f</b>	580	571	576	694	687	686	37 200	35 750	30 500	1772	1918	1736
		618	607	613	758	743	749	55 300	44 800	38 700			
		669	656	662				41 500	28 250	27 500			
8	<b>2g</b>	580	571	572	694	686	686	37 800	39 350	33 700	1720	1897	1816
		620	607	610	758	746	751	58 400	49 600	35 700			
		672	657	661				45 500	31 400	23 750			
9	<b>2h</b>	583	574	583	693	684	688	23 250	27 000	22 800	1673	1800	1700
		621	609	616	755	746	751	37 400	33 700	25 950			
		672	658	667				30 900	21 450	17 100			
10	<b>2i</b>	581	572	570	695	685	689	37 800	41 500	33 100	1766	1849	2015

		619	608	605	758	748	751	56 700	51 150	25 650			
		670	656	674				43 700	31 650	14 100			
11	<b>2j</b>	580	572	577	697	687	691	38 700	44 700	35 300			
		620	608	612	758	749	746	58 600	56 000	38 700	1782	1891	1868
		671	657	667				45 350	35 350	25 800			
12	<b>2k</b>	581	573	573	693	687	691	37 650	40 600	19 250			
		619	609	612	757	747	749	57 100	51 000	20 800	1725	1864	1868
		671	658	656				44 150	32 500	17 400			
13	<b>2l</b>	581	571	573	694	685	690	39 100	43 350	37 050			
		619	606	610	753	742	748	60 100	53 000	35 250	1746	1903	1900
		671	655	665				47 300	32 300	21 950			
14	<b>2m</b>	579	571	573	690	683	691	34 550	39 100	37 900			
		619	607	607	756	745	748	54 400	47 550	35 250	1662	1833	2003
		672	655	662				43 250	28 900	21 600			
15	<b>2n</b>	580	571	574	693	681	692	36 400	44 600	36 400			
		618	607	611	760	745	747	55 100	54 050	37 000	1751	1790	1916
		670	655	655				42 750	32 700	22 900			
16	<b>2o</b>	585	573	577	697	684	688	15 800	20 900	18 500			
		624	610	613	761	747	749	27 050	27 000	23 000	1678	1773	1778
		677	658	665				25 500	17 950	15 900			
17	<b>12</b>	724	717	724	738	736	738	194 100	163 550	131 850	262	360	262